 DOI: 10.1002/eji.201847797 Eur. J. Immunol. 2019. 49: 724–736

Basic

European Journal of Immunology

Tissue immunology and leukocyte trafficking

Research Article

Arc/Arg3.1 defines dendritic cells and Langerhans cells with superior migratory ability independent of phenotype and ontogeny in mice

Joseph Tintelnot[*1], Friederike Ufer*[*1], Jan Broder Engler*[1], Hana Winkler*[1], Karsten Lücke*[2], Hans-Willi Mittrücker*[2] and Manuel A. Friese*[1]

[1] Institut für Neuroimmunologie und Multiple Sklerose, Universitätsklinikum Hamburg-Eppendorf, Hamburg, Germany
[2] Institut für Immunologie, Universitätsklinikum Hamburg-Eppendorf, Hamburg, Germany

The key function of migratory dendritic cells (migDCs) is to take up antigens in peripheral tissues and migrate to draining lymph nodes (dLN) to initiate immune responses. Recently, we discovered that in the mouse immune system activity-regulated cytoskeleton associated protein/activity-regulated gene 3.1 (*Arc/Arg3.1*) is exclusively expressed by migDCs and is a central driver of fast inflammatory migration. However, the frequency of Arc/Arg3.1-expressing cells in different migDC subsets and Langerhans cells (LCs), their phylogenetic origin, transcription factor dependency, and functional role remain unclear. Here, we found that Arc/Arg3.1$^+$ migDCs derived from common DC precursors and radio-resistant LCs. We detected Arc/Arg3.1$^+$ migDCs in varying frequencies within each migDC subset and LCs. Consistently, they showed superiority in inflammatory migration. Arc/Arg3.1 expression was independent of the transcription factors *Irf4* or *Batf3* in vivo. In intradermal *Staphylococcus aureus* infection that relies on inflammatory antigen transport, *Arc/Arg3.1* deletion reduced T-cell responses. By contrast, Arc/Arg3.1 deficiency did not hamper the immune response to systemic *Listeria monocytogenes* infection, which does not require antigen transport. Thus, Arc/Arg3.1 expression is independent of ontogeny and phenotype and although it is restricted to a small fraction within each migDC subset and LCs, Arc/Arg3.1$^+$ migDCs are important to facilitate infectious migration.

Keywords: Cell trafficking · Dendritic cells · Immune response · Migration · Skin

Additional supporting information may be found online in the Supporting Information section at the end of the article.

Introduction

Migratory dendritic cells (migDCs) play a central role in shaping adaptive immune responses. They reside in peripheral tissues, where they constantly probe their environment, take up antigens, migrate to draining lymph nodes (dLN), and initiate T cell-driven immune responses [1–3]. Based on surface marker expression, skin-resident DCs (skinDCs), and Langerhans cells (LCs) are

Correspondence: Prof. Manuel A. Friese
e-mail: manuel.friese@zmnh.uni-hamburg.de

*These authors contributed equally to this work.

separated into at least five distinct subsets, each of which might excel in specific immunological functions [4–7]. Once migrated to the skin-draining LN (sdLN), they are referred to as migDCs. Ontogeny studies revealed that four of these five subsets, namely CD103$^+$langerin$^+$ (CD103$^+$DC) and CD103$^-$langerin$^+$ DCs (CD103$^-$DC), CD11b$^+$DCs, and double negative DCs (CD24$^-$CD11b$^-$; dnDC) derive from common hematopoietic DC precursors (CDP), depend on Fms-related tyrosine kinase 3 ligand (Flt3L) and are constantly replenished from the bone marrow [8–13]. However, approximately 5% of the CD11b$^+$DC subset is monocyte-derived. These monocyte-derived DCs (moDCs) can be further classified by surface marker expression of Ly6C, CD64, and CCR2 [1]. In contrast, LCs exclusively reside in the epidermis and constantly self-renew in situ. LCs are already established during embryogenesis from yolk sac and liver-derived precursors [14]. Experimentally, LCs can be separated from other migDCs in vivo due to their radio resistance [15].

Since DCs and especially migDCs are rare cells, challenging to isolate and difficult to culture, much insight into DC biology and function has been gained from studies on ex vivo bone-marrow derived DCs (BMDCs) [16, 17]. Recently, gene expression analysis showed that bone-marrow cultures supplemented with GM-CSF contain a subset termed "GM-DCs" that closely resemble migDCs and can be derived from CDPs in contrast to the more monocyte resembling remaining BMDCs that derive from common monocyte precursors (cMOPs) or monocyte-DC precursors (MDPs) [18–21]. Further, Flt3L supplemented bone-marrow cultures resemble classical spleen resident CD8$^+$ and CD8$^-$ DCs and to lower extent plasmacytoid DCs (pDCs) while M-CSF supplemented cultures lead to generation of macrophages [5, 18]. Moreover, differentiation of hematopoietic progenitors into distinct migDC subsets is tightly regulated by lineage-determining transcription factors [22]. Thus, development of CD103$^+$DCs and CD103$^-$DCs (also referred to as cDC1) [23] depend on basic leucine zipper transcription factor ATF-like 3 (*Batf3*), whereas development or migration of other DCs such as CD11b$^+$ DCs or dnDCs (also referred to as cDC2) depend on the transcription factor interferon-regulatory factor 4 (*Irf4*) [24–26].

Classifying DCs is mandatory to secure experimental comparability and to exploit subset-specific functions in vaccination and autoimmunity [4, 7]. However, integration of the manifold findings from cell surface expression analysis, ontogeny studies, and transcriptional dependencies did so far not result in a satisfying classification of DCs and in particular migDCs in sdLNs and LCs. To harmonize DC experiments, a new DC classification has been proposed, based on ontogeny in combination with function, phenotype, and localization [27, 28]. Yet, to overcome the complex heterogeneity, more functional markers are required to allow the transition from a DC classification based on phenotype to one that appreciates biological in vivo function. We have recently provided experimental support for this functional approach by identifying the activity-regulated cytoskeleton associated protein/activity-regulated gene 3.1 (*Arc/Arg3.1*) in the immune system. We could show that Arc/Arg3.1 expression is strictly confined to migDCs or LC and is required for an accelerated DC migration in vitro and in vivo [29]. Notably, we found Arc/Arg3.1 to be stably expressed upon stimulation. However, it is unknown whether Arc/Arg3.1 characterizes all skinDCs and LCs or whether Arc/Arg3.1 is confined to certain migDC or LC subsets in sdLN.

Here, we discovered that Arc/Arg3.1 expression is detectable only in a small fraction of cells in each DC and LC subset in skin and migDC and LC subset in sdLN. Arc/Arg3.1$^+$ cells were equipped with superior migratory capacity and were indispensable for mounting proper T-cell responses in a model of skin infection. We found that Arc/Arg3.1$^+$ migDCs and LCs are independent of canonical transcription factors and do not share a distinct ontogeny.

Results

All migDC subsets and LCs depend on Arc/Arg3.1 for fast inflammatory migration

To investigate Arc/Arg3.1 expression in migDCs and LCs [3, 30], we used *Arc/Arg3.1*^{eGFP} mice [31], which express enhanced eGFP under the control of the *Arc/Arg3.1* promoter. In sdLN, we found approximately 20% (17.7 ± 5.4%) of total migDCs and LCs to express Arc/Arg3.1 under steady-state conditions (Fig. 1A and Supporting Information Fig. 1A for gating strategy). Notably, we detected a substantial amount of Arc/Arg3.1-expressing cells in each subset (Fig. 1A), while the Arc/Arg3.1-positive fraction varied between approximately 10% in CD11b$^+$DC and almost 40% in the combined cluster of CD103$^-$DC and LCs (35.5 ± 8.7%; Fig. 1A). The monocyte marker Ly6C was expressed by approximately 5% (4.5 ± 1.4%) of Arc/Arg3.1$^+$ migDCs and did show comparable frequencies in Arc/Arg3.1$^-$ migDCs (Supporting Information Fig. 1B). Expression of activation markers CD40, CD80, and CD86 was also comparable between Arc/Arg3.1-eGFP$^+$ and Arc/Arg3.1-eGFP$^-$ migDCs (Supporting Information Fig. 1C). Next, we explored the functional impact of Arc/Arg3.1 on fast inflammatory migration in the different migDC subsets and LCs. Since skinDCs migrate to the dLN after skin sensitization, we applied tetramethyl rhodamine isothiocyanate (TRITC) in an organic solvent on ear-skin of *Arc/Arg3.1*^{eGFP} mice and analyzed TRITC$^+$ cells in draining auricular LN after 72 hours [32, 33]. Focusing on TRITC-positive DCs, we detected approximately twice as many TRITC$^+$ cells in Arc/Arg3.1-positive migDCs compared to TRITC$^+$ cells in Arc/Arg3.1-negative migDCs ($p = 0.011$; Fig. 1B) and could indeed observe a superior migratory capacity of Arc/Arg3.1$^+$ migDCs compared to Arc/Arg3.1-negative migDCs in all subsets ($p = 0.011$ for CD11b$^+$DC, $p = 0.02$ for CD103$^+$DC, $p = 0.011$ for CD103$^-$DC + LC and $p = 0.033$ for dnDC; Fig. 1C). We obtained similar results 48 hours after ear-skin painting (Supporting Information Fig. 1D and E) and observed a trend as early as 24 hours after sensitization (Supporting Information Fig. S1F). Notably, we could not detect any TRITC$^+$ cells in nondraining LN, confirming that the transport of TRITC to draining LN was due to migration and not circulating particles ($p < 0.001$; Supporting Information Fig. 1G). During experimental recording,

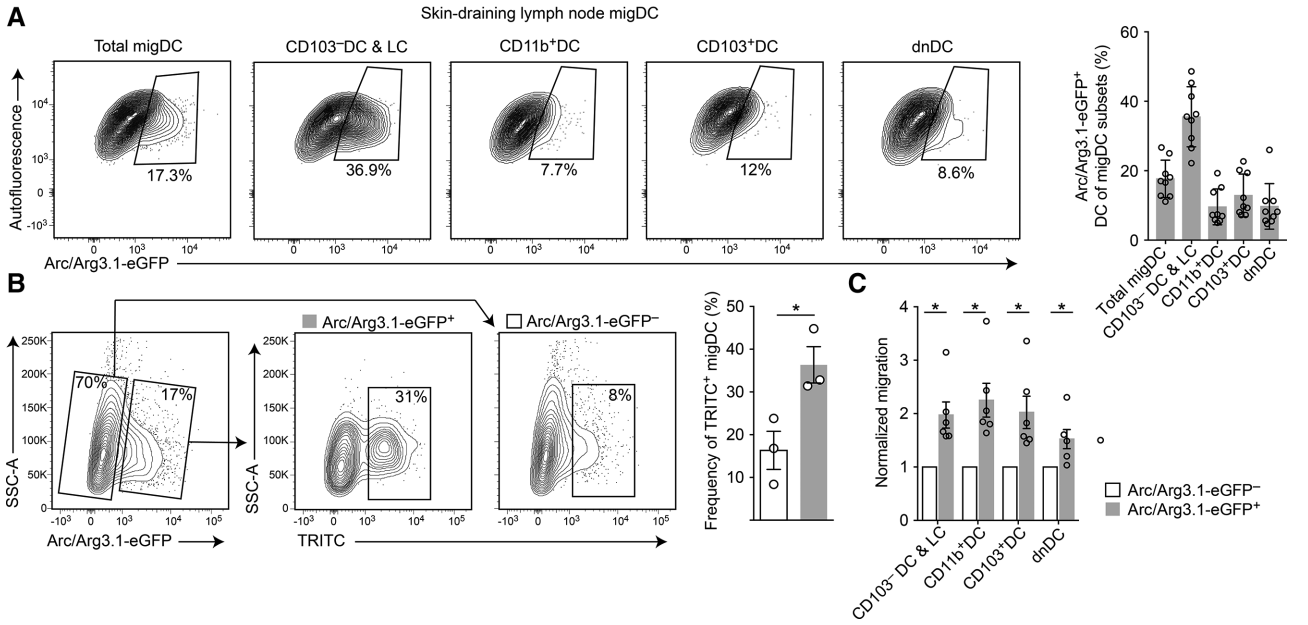

Figure 1. Arc/Arg3.1 is expressed by all migDC subsets and LCs in sdLN. (A) Flow cytometry analysis of Arc/Arg3.1 expression in indicated migDC subsets and LCs from sdLN of naïve *Arc/Arg3.1*^{eGFP} mice and quantification (right). Pooled data from three independent experiments with three mice each. Mean ± SEM. (B, C) Flow cytometry analysis of TRITC$^+$ migDCs and LCs from draining auricular LN 72 hours after TRITC ear-skin painting in *Arc/Arg3.1*^{eGFP} mice. (B) Bar plot shows TRITC$^+$ migDCs and LCs among Arc/Arg3.1-eGFP$^+$ and Arc/Arg3.1-eGFP$^-$ migDCs. One out of two experiments with three mice each. Mean ± SEM. (C) Normalized migration for depicted TRITC$^+$ Arc/Arg3.1-eGFP$^+$ subset was calculated relative to percentage of TRITC$^+$ cells among Arc/Arg3.1-eGFP$^-$ CD11c$^+$MHC-II^{high} cells that was set to 1. Pooled from two individual experiments with three mice each. Mean ± SEM. Two-tailed Student's *t*-test (B) and one-sample *t*-test against 1 (C); $^*p < 0.05$.

subset-specific Arc/Arg3.1 expression was stable among all subsets, which allowed us to exclude an inflammation-mediated Arc/Arg3.1 induction (Supporting Information Fig. 1H). Taken together, these results indicate that Arc/Arg3.1-positive migDCs are found in all migDC subsets and LCs and are uniquely equipped with superior migratory capacities.

Arc/Arg3.1$^+$ DCs and LCs in the skin are replenished via different routes

Previously tested inflammatory stimuli and stressors did not induce Arc/Arg3.1 mRNA or protein expression in fully differentiated Arc/Arg3.1-negative DCs, nor could we enhance Arc/Arg3.1 expression levels in Arc/Arg3.1-positive DCs [29]. Following up on this, we next explored the source of Arc/Arg3.1-positive DCs in sdLN. All migDCs and LCs recovered from sdLN are thought to have influxed from the skin. Therefore, we analyzed Arc/Arg3.1 expression in DCs and LCs directly recovered from the skin of *Arc/Arg3.1*^{eGFP} mice and found approximately 8% (7.9 ± 2.1%) of total skinDCs to express Arc/Arg3.1 during steady-state contained within all subsets (Fig. 2A and Supporting Information Fig. 2A for gating strategy). Among all analyzed cells, LCs showed the highest share of Arc/Arg3.1-positive cells (10.8 ± 2.1%; Fig. 2A). Since LCs are localized exclusively in the epidermis, we could distinguish them from other skinDCs by processing dermis and epidermis separately (Supporting Information Fig. 2B).

Having shown that Arc/Arg3.1$^+$ migDCs and LCs are already present in the skin, we next explored the source of their replenishment. Therefore, we analyzed the reappearance of migDCs and LCs in sdLN after ablation of radio-sensitive cells. We transferred congenic CD45.2$^+$ *Arc/Arg3.1*^{eGFP} bone marrow into sublethally irradiated WT CD45.1 mice (Supporting Information Fig. 2C and D) and indeed observed a replenishment of Arc/Arg3.1$^+$ DCs to steady-state levels from donor cells in all migDC subsets after six weeks (Fig. 2B, Supporting Information Fig. 2E). In line with previous studies [15], LCs were not replenished from CD45.2 *Arc/Arg3.1*^{eGFP} donor bone marrow but remained of CD45.1 host origin (Fig. 2B). To proof the independent self-renewal of Arc/Arg3.1$^+$ LCs, we transferred WT CD45.1 bone marrow into sublethally irradiated CD45.2 *Arc/Arg3.1*^{eGFP} mice. In this alternative setup, we found the sole remaining CD11c$^+$MHC-II^{high} cells of host origin in the sdLN to be LCs and more than one third of them (39 ± 9.9%) expressing Arc/Arg3.1 (Fig. 2C). Thus, both in dermis and epidermis Arc/Arg3.1-positive DCs are found in all DC subsets and LCs. In the dermis, they are continuously replenished from bone marrow precursor cells, while radio-resistant Arc/Arg3.1$^+$ LCs rely on independent self-renewal.

Arc/Arg3.1$^+$ is induced with differentiation in classical DC precursors

As we found Arc/Arg3.1$^+$ migDCs to replenish from the bone marrow after transplantation, we next asked whether myeloid

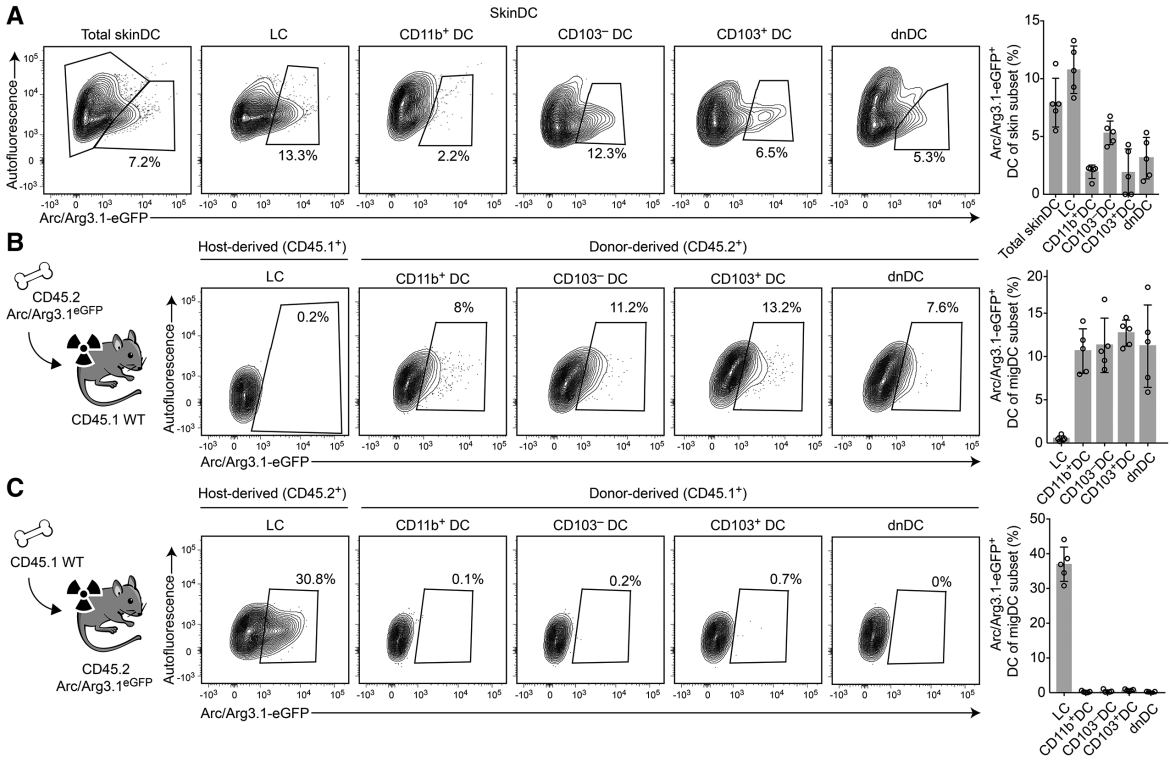

Figure 2. Self-renewing LCs and bone marrow-derived migDCs express Arc/Arg3.1 in skin and sdLN. (A) Flow cytometry analysis of Arc/Arg3.1 expression in indicated skinDC or LC subsets from naïve *Arc/Arg3.1*^{eGFP} mice and quantification (right). Pooled data from two independent experiments with three mice each. Mean ± SEM. (B) Flow cytometry analysis of Arc/Arg3.1 expression in indicated migDC subsets or LCs from sdLN of CD45.1 WT mice six weeks after transfer of CD45.2 *Arc/Arg3.1*^{eGFP} donor bone marrow into sublethally irradiated CD45.1 WT hosts and quantification (right). Pooled data from two individual experiments with two to three mice each. Mean ± SEM. (C) Flow cytometry analysis of Arc/Arg3.1 expression in indicated migDC subsets or LCs from sdLN of CD45.2 *Arc/Arg3.1*^{eGFP} mice six weeks after transfer of CD45.1 WT donor bone marrow into sublethally irradiated CD45.2 *Arc/Arg3.1*^{eGFP} hosts and quantification (right). Pooled data from two individual experiments with two to three mice each. Mean ± SEM.

progenitor cells in naïve bone marrow (MDPs and CDPs) already express Arc/Arg3.1. Notably, no Arc/Arg3.1 expression was observed in CDPs or MDPs (Fig. 3A). However, when we cultured bone marrow in the presence of GM-CSF we observed a gradual increase of *Arc/Arg3.1* mRNA that peaked at day seven ($p < 0.001$ for day 2–4 and day 4–6, $p = 0.009$ for day 6–7 and $p = 0.003$ for day 7–10; Fig. 3B). In contrast, only negligible small numbers of Arc/Arg3.1$^+$ cells were generated in culture supplemented with Flt3L or M-CSF ($p < 0.001$ for both; Fig. 3C). Culturing naïve BM from *Arc/Arg3.1*^{eGFP} mice showed similar results and revealed that only a small fraction of the GM-CSF generated BMDCs expressed Arc/Arg3.1, somewhat resembling the situation in vivo with only a fraction of migDCs being Arc/Arg3.1$^+$ (Supporting Information Fig. 3A and B). More than 90% of Arc/Arg3.1-positive BMDCs were CD11b^{intermediate}MHC-II^{high} with some of them being CD115$^-$CD135$^+$ (GM-DCs according to [19]) transcriptionally resembling migDCs (Supporting Information Fig. 3C and D). In contrast, Arc/Arg3.1-negative BMDCs are predominantly comprised of MHC-II^{low} cells including CD11b^{high} cells that are presumed to be macrophage-like cells ($p < 0.001$; Fig. S2C) [19]. Of note, in vivo injection of GM-CSF subcutaneously in WT mice did not increase relative frequencies of Arc/Arg3.1$^+$ migDCs or LCs in sdLNs (Supporting Information Fig. 3E).

To identify the progenitor population that gives rise to Arc/Arg3.1$^+$ DCs, we purified MDPs, CDPs, and common monocyte precursors (cMOPs) from CD45.2 *Arc/Arg3.1*^{eGFP} bone marrow and cultured them in the presence of naïve bone marrow from CD45.1 WT mice as feeder cells. Consistent with previous results [19, 20], MDPs and cMOPs proliferated well in GM-CSF cocultures, in contrast CDPs proliferated markedly less (Supporting Information Fig. 3F). Notably, we found Arc/Arg3.1$^+$ BMDCs to derive from all three precursors at significantly higher frequencies compared to total *Arc/Arg3.1*^{eGFP} bone marrow ($p = 0.048$ for CDP, $p = 0.005$ for MDP and $p = 0.033$ for cMOP; Fig. 3D). Additionally, they showed a more pronounced MHC-II^{high} phenotype compared to total bone marrow cultures ($p < 0.001$ for CDP, $p = 0.043$ for MDP and $p = 0.017$ for cMOP; Fig. 3D). In BMDCs generated from *Flt3l*$^{-/-}$ mice, which show already a reduction of DC progenitors in bone marrow [11], we also detected a reduced *Arc/Arg3.1*$^+$ mRNA expression compared to WT BMDCs (Supporting Information Fig. 3G).

To translate our results in vivo, we injected Arc/Arg3.1-negative CDPs isolated from bone marrow of CD45.2 *Arc/Arg3.1*^{eGFP} mice intrafemorally into CD45.1 WT mice. Four days after transfer, we detected donor-derived CD45.2$^+$Arc/Arg3.1$^+$ cells in sdLN showing a clear CD11c$^+$

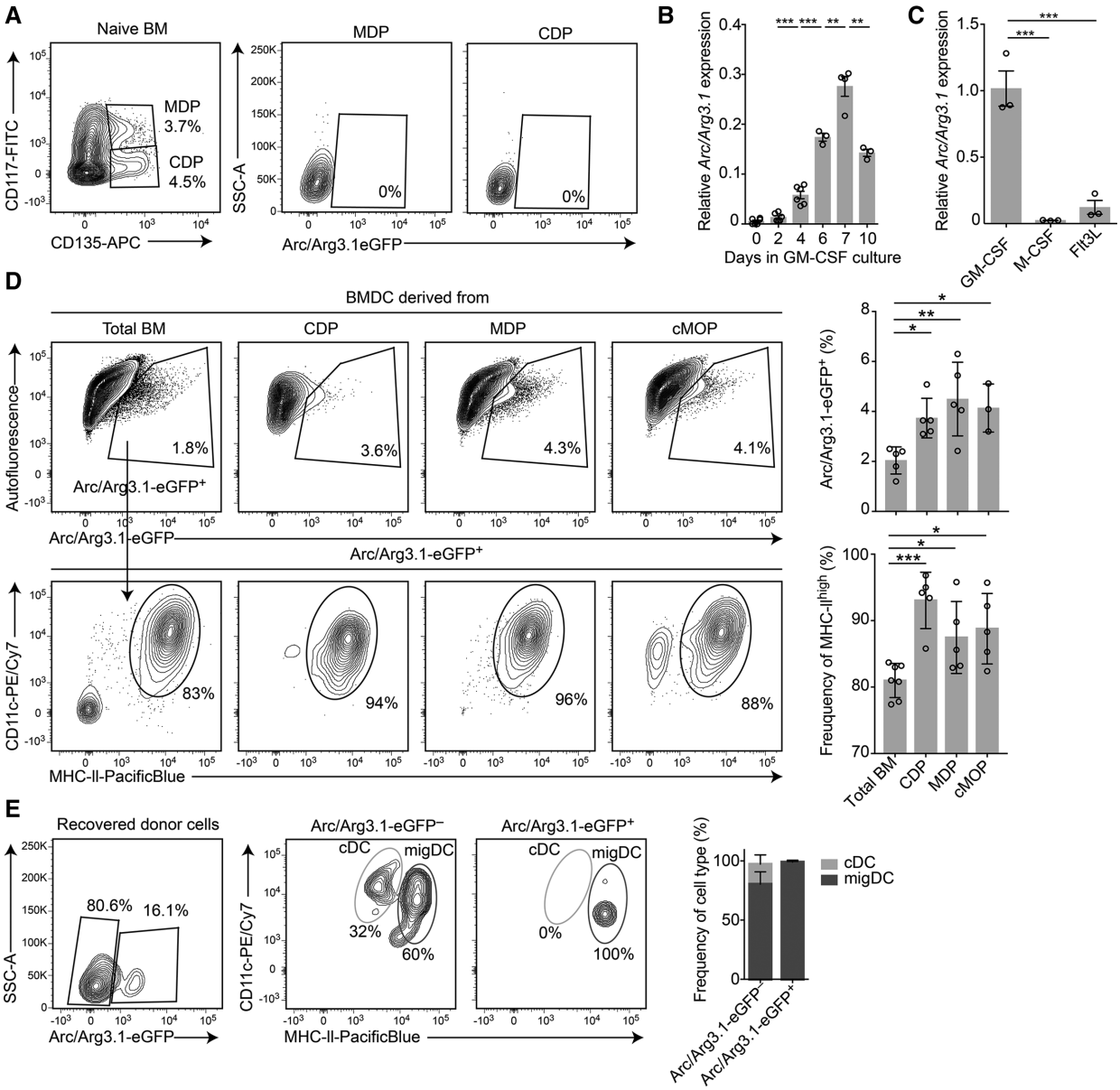

Figure 3. Arc/Arg3.1$^+$ DCs derive from Arc/Arg3.1$^-$ DC precursors in vivo and in vitro. (A) Flow cytometry analysis of Arc/Arg3.1-eGFP$^+$ expression in naïve bone marrow (Lin$^-$CD11b$^-$MHCII$^-$CD11c$^-$CD115$^+$) gated on MDP (CD117$^+$CD135$^+$) and CDP (CD117$^+$CD135$^+$) of *Arc/Arg3.1*^{eGFP} mouse. Representative example from one experiment out of three with three mice each. (B) Relative *Arc/Arg3.1* mRNA expression of WT bone marrow cultured in GM-CSF supplemented medium. One out of two individual experiments with three to six mice each. Mean ± SEM. (C) Relative *Arc/Arg3.1* mRNA expression of BMDCs cultured in the presence of indicated cytokine in vitro. One out of two individual experiments with three mice each. Mean ± SEM. (D) Sorted CDPs, MDPs, or cMOPs from CD45.2$^+$ *Arc/Arg3.1*^{eGFP} bone marrow (BM) were cocultured with complete CD45.1 WT BM. Cultured total CD45.2 *Arc/Arg3.1*^{eGFP} BM was used as control. Flow cytometry analysis shows frequency of Arc/Arg3.1-eGFP$^+$ BMDCs (left) and among those frequencies of MHC-II^{high} BMDCs (right) at day six of culture. Pooled data from three individual experiments with one to two mice each. Mean ± SEM. (E) Fluorescently isolated Arc/Arg3.1-eGFP$^-$ CDP from CD45.2 *Arc/Arg3.1*^{eGFP} bone marrow were injected intrafemorally in CD45.1 WT mice. Flow cytometry analysis of recovered donor cells from sdLN. Stack bar plot shows distribution of recovered Arc/Arg3.1-eGFP$^+$ and Arc/Arg3.1-eGFP$^-$ donor cells among DC subsets. Pooled data from three individual experiments. Mean ± SEM. Two-tailed Student´s *t*-test (B). One-way ANOVA followed by a Dunnett post hoc test for multiple comparisons (C, D); $^*p < 0.05$, $^{**}p < 0.01$, and $^{***}p < 0.001$.

MHC-II^{high} migDC phenotype (Fig. 3E). These results suggest that Arc/Arg3.1$^+$ BMDCs directly develop out of Arc/Arg3.1$^-$ DC and monocyte precursors from naïve bone marrow in vitro. Similarly, Arc/Arg3.1$^+$ migDCs develop out of Arc/Arg3.1$^-$ DC precursors in vivo.

Arc/Arg3.1$^+$ migDCs are heterogeneous in their transcription factor dependency

Since *Batf3* and *Irf4* have been shown to be important transcription factors for migDC development, we next asked whether

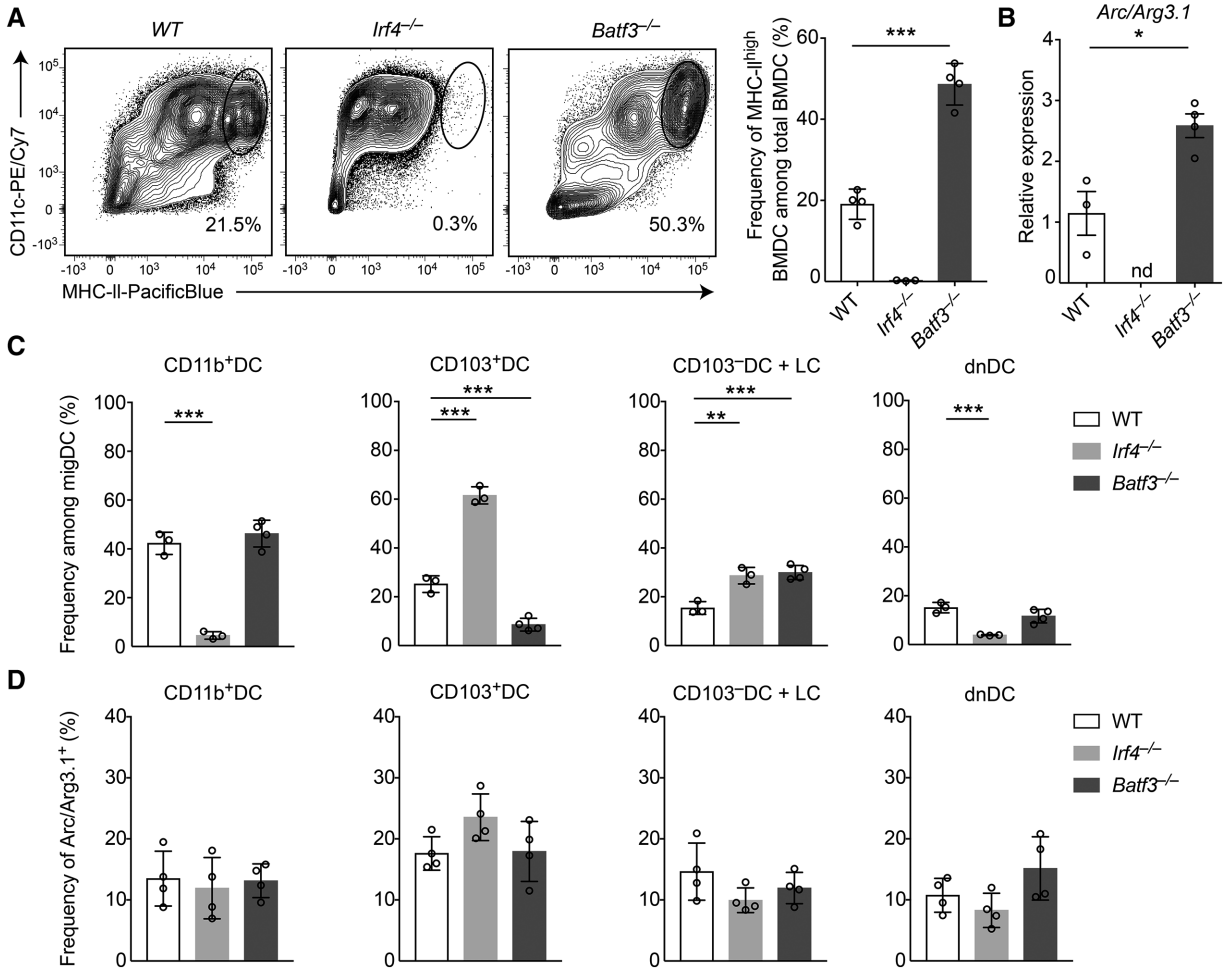

Figure 4. Arc/Arg3.1$^+$ migDCs do not depend on *Batf3* or *Irf4* in vivo. (A) Flow cytometry analysis of BMDCs from WT, *Irf4*$^{-/-}$ or *Batf3*$^{-/-}$ mice. Bar plot shows frequency of MHCII^{high} BMDCs. One out of two independent experiments with three to four mice each. Mean ± SEM. (B) Relative *Arc/Arg3.1* mRNA expression of BMDCs from indicated mouse strains. One experiment out of two with three mice each. Mean ± SEM; not detected (nd). (C, D) Flow cytometry analysis of (C) indicated migDC subset frequency among total migDCs and (D) Arc/Arg3.1$^+$ migDC frequency of indicated migDC subset from sdLN of WT, *Irf4*$^{-/-}$ and *Batf3*$^{-/-}$ mice (using Arc/Arg3.1-antibody). One experiment out of two with three to four mice each. Mean ± SEM. Two-tailed Student´s *t*-test (A, B). One-way ANOVA followed by a Dunnett post hoc test for multiple comparisons (C, D); $^*p < 0.05$, $^{**}p < 0.01$, and $^{***}p < 0.001$.

Arc/Arg3.1$^+$ migDCs depend on these canonical transcription factors. We analyzed their influence on Arc/Arg3.1-expression in BMDCs in vitro and migDCs from sdLN in vivo. In line with published data [26, 34], we found in vitro generated MHC-II^{high} BMDCs to be highly dependent on *Irf4*, as we were unable to generate MHC-II^{high} BMDCs from bone marrow of *Irf4*$^{-/-}$ mice (Fig. 4A). Of note, the absence of MHC-II^{high} BMDCs coincided with the absence of *Arc/Arg3.1* mRNA in GM-CSF cultures from *Irf4*$^{-/-}$ mice (Fig. 4B). By contrast, BMDC cultures from *Batf3*$^{-/-}$ mice showed a relative increase of MHC-II^{high} BMDCs compared to WT cultures ($p < 0.001$; Fig. 4A), which was again reflected in an increase of *Arc/Arg3.1* mRNA expression ($p = 0.012$; Fig. 4B). To analyze transcription factor dependency of Arc/Arg3.1-migDCs in vivo, we first established a specific Arc/Arg3.1-antibody staining for flow cytometry (Supporting Information Fig. 4A and Supporting Information 4B). When we compared our results from Fig. 1A for *Arc/Arg3.1*^{eGFP} mice regarding subset distribution of Arc/Arg3.1-positive migDCs, we obtained similar results by staining with an antibody directed against Arc/Arg3.1 in WT mice (Supporting Information Fig. 4C). In our hands, *Irf4*$^{-/-}$ mice showed significantly reduced CD11b$^+$DC (cDC2) and dnDC in sdLN (both $p < 0.001$; Fig. 4C) [24], whereas *Batf3*$^{-/-}$ mice showed drastically reduced CD103$^+$DC (cDC1) ($p < 0.001$; Fig. 4C) [23]. At the same time, we found a relative enrichment of CD103$^+$DCs, CD103$^-$DCs, and LCs in *Irf4*$^{-/-}$ mice ($p < 0.001$ for CD103$^+$DCs and $p = 0.002$ for CD103$^-$DC/LC; Fig. 4C). Although the relative contribution of the different migDC subsets depended on the presence of *Irf4* and *Batf3*, the percentage of Arc/Arg3.1$^+$ DCs in each population was not affected by the absence of *Irf4* or *Batf3* (Fig. 4D and Supporting Information Fig. 4D for gating control). Consistently, the total frequency of Arc/Arg3.1-positive migDCs and LCs was comparable between WT, *Irf4*$^{-/-}$, *Batf3*$^{-/-}$mice (Supporting Information Fig. 4E). When we analyzed *Flt3l*$^{-/-}$ mice, we could recapitulate the reduction in cDC1 and cDC2 (Supporting

Information Fig. 4F) [8]. However, relative Arc/Arg3.1 expression was not affected (Supporting Information Fig. 4G). Thus, in vitro Arc/Arg3.1$^+$ BMDCs were dependent on the transcription factor Irf4, while in vivo the frequency of Arc/Arg3.1$^+$ DCs inside the migDC subsets was not changed in the absence of *Irf4*, *Batf3,* or *Flt3l*.

Arc/Arg3.1$^+$ DCs and LCs mount T-cell response in cutaneous *Staphylococcus aureus* infection

To explore the functional role of Arc/Arg3.1-dependent DC and LC migration in vivo, we applied two different infection models, resembling either local or systemic bacterial infection. First, we infected the skin of *Arc/Arg3.1*$^{-/-}$ mice and WT controls with 1–2 $\times$ 10^6 CFU *Staphylococcus aureus*, an intermediate microbial burden that is sufficient to induce visible wounds [35, 36]. Four days after infection, absolute leukocyte numbers in sdLN were significantly reduced in *Arc/Arg3.1*$^{-/-}$ mice compared to WT littermates ($p < 0.001$; Fig. 5A). This effect was mainly driven by a marked reduction of T cells and migDCs and LCs (both $p < 0.001$, Fig. 5B). In the absence of Arc/Arg3.1 all migDC subsets and LCs except dnDCs were significantly reduced. ($p < 0.001$ for CD103$^-$+LCs and CD11b$^+$DCs, $p = 0.02$ for CD103$^+$ DCs and $p = 0.46$ for dnDCs; Fig. 5C.) Further analysis revealed a reduction of activated (CD44$^+$) as well as IFN-γ-producing CD4$^+$ and CD8$^+$ T cells in the absence of *Arc/Arg3.1* ($p < 0.001$ for CD4$^+$CD44$^+$ T cells, $p = 0.024$ for CD8$^+$CD44$^+$ T cells, $p = 0.02$ for CD4$^+$IFN-γ$^+$, $p = 0.018$ for CD8$^+$IFN-γ$^+$; Fig. 5D and E). In contrast, numbers of IL-17A-producing CD4$^+$ (TH17) or CD8$^+$ (CD8$^+$IL17$^+$) T cells (Supporting Information Fig. 5A) and the size of skin lesions did not depend on *Arc/Arg3.1* (Fig. 5F). Importantly, we could rule out a priori steady-state differences in composition and numbers of DCs in skin and sdLN in *Arc/Arg3.1*$^{-/-}$ mice (Supporting Information Fig. 5B–D). Likewise, T-cell stimulation capacity did not depend on Arc/Arg3.1, when we used Ova-specific CD4$^+$ and CD8$^+$ T cells and stimulated them with Arc/Arg3.1-eGFP$^+$ and Arc/Arg3.1-eGFP$^-$ BMDCs. (Supporting Information Fig. 5E and F). Together, our results indicate a pronounced impairment of the T-cell response to local bacterial infection in *Arc/Arg3.1*$^{-/-}$ mice. Since this model depends upon an effective antigen uptake, processing, and presentation by migDCs and LCs, which are the only immune cells expressing *Arc/Arg3.1*, we concluded that *Arc/Arg3.1*$^+$ DCs and LCs represent a pivotal cell type responding to local infections. Next, we intravenously infected *Arc/Arg3.1*$^{-/-}$ mice and WT controls with OVA-expressing *Listeria monocytogenes*. In this model, *Arc/Arg3.1*$^{-/-}$ mice showed no difference in the induction of *L. monocytogenes*-specific CD4$^+$ and CD8$^+$ T cells in comparison to WT littermates (Supporting Information Fig. 5G), corroborating our findings that only migDCs and LCs but not lymphoid-resident DCs or T cells depend on Arc/Arg3.1. In conclusion, Arc/Arg3.1$^+$ migDCs and LCs control T-cell activation and IFN-γ production in lymphoid organs after local (skin), but not systemic (intravenous) infection.

Discussion

In this study, we show that a distinct proportion of the currently described four migDC subsets as well as LCs in the skin and sdLN expressed Arc/Arg3.1. More important, our results identified Arc/Arg3.1 as a key factor for fast inflammatory migration within each migDC subset and LCs. This functional impact of Arc/Arg3.1 is independent of ontogeny, as yolk sac-derived LCs in vivo as well as migDCs derived from different DC and monocyte precursors in vitro and DC precursors in vivo showed a stable fraction of Arc/Arg3.1-positive cells. However, since surface markers characterizing monocytes are only marginally expressed by Arc/Arg3.1-positive cells, we do not expect monocyte-derived Arc/Arg3.1-positive cells to be functionally relevant in vivo. We found no evidence for an early commitment of progenitor cells to an Arc/Arg3.1$^+$ lineage. Moreover, Arc/Arg3.1 expression was detectable among migDC subsets in both, *Batf3*$^{-/-}$ and *Irf4*$^{-/-}$ mice in vivo. This argues against a dependency of Arc/Arg3.1-positive DCs or Arc/Arg3.1 transcription on either one of those two key migDC transcription factors. In infectious models, we could underline the clinical relevance of Arc/Arg3.1-dependent migration since T-cell priming and activation after dermal challenge with *S. aureus* was impaired, while migDC-independent intravenous *L. monocytogenes* infection was not altered in *Arc/Arg3.1*$^{-/-}$ mice and no superiority in T-cell priming of Arc/Arg3.1$^+$ BMDCs was observed in vitro.

Our results support the notion, that Arc/Arg3.1-expressing DCs and LCs are not to be viewed as an independent subset but rather show that Arc/Arg3.1-expressing cells from different subsets are unified by a shared functional feature, namely fast inflammatory migration. The classification of DCs has been highly debated during recent years and a classification primarily based on ontogeny and secondarily on function, location, or phenotype has been proposed [27, 28]. Our observation, that ontogenetically different migDCs as well as LCs are equipped with shared functions fits in the most recent picture that can be concluded from the manifold studies reported in predominantly single gene manipulated mice. Individual migDC subsets or LCs [37], have been shown to often be sufficient but at the same time partly redundant for orchestrating different immune functions.

Although we could not show, at what differential state Arc/Arg3.1-positive DCs exactly branch off from concurrently existing Arc/Arg3.1-negative DCs of the respective subset, we can exclude that a tissue specific cofactor is required for differentiation, as we could generate Arc/Arg3.1-positive cells from different initially Arc/Arg3.1-negative myeloid precursors in vitro. Interestingly, the proportion of Arc/Arg3.1-expressing DCs and LCs was remarkably stable in vitro and in vivo within each subset and was also reliably replenished after bone marrow transplantation. Since neither inflammation in vivo nor different experimental stimuli in vitro [29] led to a relative increase in Arc/Arg3.1-expressing cells, one can speculate about the existence of a genetically imprinted feed-forward mechanism to prevent subset dominance or the existence of an unknown Arc/Arg3.1-specific transcription factor

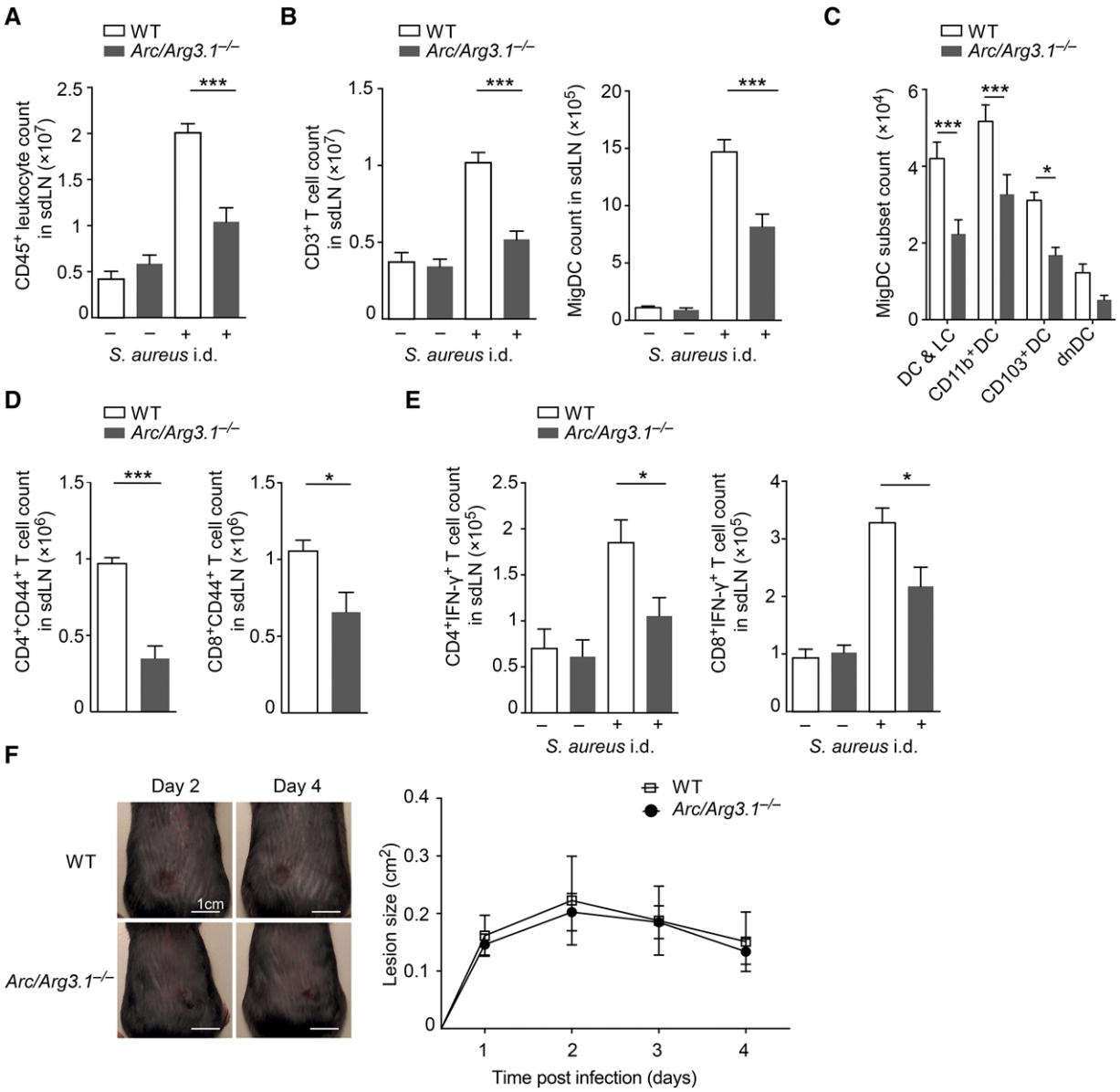

Figure 5. Arc/Arg3.1$^+$ migDCs and LCs control *Staphylococcus aureus* induced T-cell activation in sdLN. (A–E) Flow cytometry analysis of sdLN from *Arc/Arg3.1*$^{-/-}$ and WT mice four days after infection with 1–2 × 10^6 CFU *Staphylococcus aureus* or PBS intradermally. (A–D) Absolute cell counts of (A), leukocytes (B) T cells and total migDCs and LCs as well as (C) individual subsets. Pooled data from two individual experiments with four to five mice each. Mean + SEM. (D) Absolut cell counts of activated CD4$^+$ (left) and CD8$^+$ T cells (right). One experiment with five mice. Mean + SEM. (E) Absolute counts of IFN-γ-producing CD4$^+$ (left) and CD8$^+$ T cells (right). (F) Representative photographs of skin lesions from *S. aureus* i.d. infected WT and *Arc/Arg3.1*$^{-/-}$ mice (left, scale bar represents 1 cm) and statistical analysis of lesion size during course of infection (right). One out of two independent experiments with four to five mice each. Mean ± SEM. Two-tailed Student's *t*-test (A–E). Two-way ANOVA followed by a Sidak's post hoc test for multiple comparisons (F); $^*p < 0.05$ or $^{***}p < 0.001$.

with lineage-determining and simultaneously restricting capacity. Intriguingly, we observed increased frequencies of Arc/Arg3.1$^+$ migDCs in sdLN compared to the frequencies of Arc/Arg3.1$^+$ skinDCs. This might be explained by their supremacy in migration, which could simply lead to an accumulation of Arc/Arg3.1$^+$ migDCs and LCs in sdLN. Alternatively, an induction of Arc/Arg3.1 in skinDCs and LCs following an unknown stimulus in the context of maturation right before leaving the skin is still possible. This difference in Arc/Arg3.1-positive cell numbers might also be part of a constant niche competition as it has been proposed for macrophages [38].

DC and LC migration is required for most DC/LC-driven immune responses [39]. Previously, we reported that Arc/Arg3.1$^+$ DCs are important for autoimmune reactions [25]. In infections, the clinical relevance of Arc/Arg3.1-facilitated DC migration is now highlighted by our observation of drastically reduced immune response in *Arc/Arg3.1*$^{-/-}$ mice compared to WT littermates after local skin infection with *S. aureus*. Strikingly, migDCs and LCs

themselves as well as IFN-γ-producing $CD4^+$ and $CD8^+$ T cells, which are induced by intradermal bacterial challenge [5], were strongly reduced, although Arc/$Arg3.1^+$ migDCs and Arc/$Arg3.1^+$ LCs are a minority within each subset. We found no differences in IL-17A-producing $CD4^+$ and $CD8^+$ T cells, both of which are mainly induced by migDC-independent noninflammatory skin colonization [5, 40]. However, we found no difference in wound exacerbation between genotypes. This might be due to the previously reported observation, that local bacteria clearance in this model is performed by neutrophils [41, 42], which are unaltered in the absence of Arc/Arg3.1 [29]. In contrast, we found an unaltered immune response in *Arc/Arg3.1*$^{-/-}$ mice after systemic challenge with *L. monocytogenes*. This underlines the specific importance of Arc/Arg3.1 in DC migration, since this systemic bacterial infection is largely independent of peripheral antigen uptake and effective delivery to the LN and instead relies on spleen-resident $CD8^+$ DCs [43, 44]. From observing an unaltered T-cell response in *L. monocytogenes* infection, we can also exclude a T-cell intrinsic defect in the absence of Arc/Arg3.1.

In summary, our results present first evidence for a potential functional homogeneity in migration that is shared among heterogeneous migDCs and LCs, differing in ontogeny, phenotype, and transcriptional regulation. Thereby, Arc/Arg3.1-although only expressed in a minority of migDCs and LCs-presents as a highly important factor in mounting immune responses by all subsets depending on migration. How exactly these broad effects for immune responses can be facilitated by this rather rare fraction of Arc/$Arg3.1^+$ DCs and LCs remains to be investigated.

Methods

Mice

We purchased C57BL/6 and B6.SJL-*Ptprc*^{a} *Pepc*^{b}/BoyJ (CD45.1) mice from The Jackson Laboratory (Maine, USA). *Arc/Arg3.1*$^{-/-}$ [45], *Irf4*$^{-/-}$ [46], *Batf3*$^{-/-}$ [23], *Flt3l*$^{-/-}$[47], OT-I [48], OT-II [49], and *Arc/Arg3.1*^{eGFP} transgenic [31, 50] mice were previously described. We bread mice under pathogen-free conditions. We used gender- and age-matched mice between 4 and 16 weeks of age for each experiment, with respective littermate controls on a C57BL/6 background. When possible, we performed preliminary experiments to determine requirements for sample size in order to minimize animal numbers. Animals were assigned randomly to experimental groups. All experiments were approved by the local ethics committee (*Behörde für Soziales, Familie, Gesundheit und Verbraucherschutz in Hamburg*; 81/015, G68/11, and Org713).

Cell preparation and culture condition

We isolated cells from spleen and bone marrow as previously described [51]. We obtained DCs from skin-draining lymph node (sdLN) by first mechanically disrupting the tissue before digesting in 1.25 mg/mL collagenase D (Roche) and 50 μg/mL DNase I (Roche) for 35 min gently shaking at 37°C, adding 10 μM EDTA (Sigma-Aldrich) for the last five minutes. After homogenizing the tissue through a 40 μm cell strainer (Greiner) and washing with ice-cold PBS, we pelleted cells (300 × g, 7 min, 4°C). For cell culturing, we used mouse complete medium (10% FCS, 50 μM 2-mercaptoethanol, 100 U/mL penicillin/streptomycin in RPMI1640). We obtained skin DCs as described before [52]. In brief, we cut ears into two halves using forceps and incubated split-side down in 2 mL 1 mg/mL dispase ll (Sigma-Aldrich) overnight at 4°C. After mechanically disrupting the tissue using scissors, we digested the tissue in 1.25 mg/mL collagenase D (Roche) for 90 min at 37°C. After digestion, we homogenized the cell suspension through a 40 μm cell strainer (Greiner) and washed with PEF (PBS, 10% FCS and 1% EDTA).

Generation of BMDCs

We obtained bone marrow from 6 to 12 weeks old mice as described before [16]. In brief, we homogenized cells through 40 μm cell strainers (Greiner) and incubated them in red blood cell lysis buffer (0.15 M NH_4Cl, 10 mM $KHCO_3$, 0.1 mM Na_2EDTA in ddH_2O at pH 7.4) for 5 min. We washed cells in PBS (PAN Biotech), counted them and i.v. injected cells for mixed bone marrow chimeras, stained them for flow cytometry analysis of naïve bone marrow or cultured them in the presence of growth factors for the generation of BMDC. GM-CSF-induced BMDC were generated by culturing BMDC in 100 mL cell culture flasks (Sarstedt) for standard experiments or 12 well-plates (Sarstedt) for coculture experiments in mouse complete medium containing 20 ng/mL GM-CSF (PeproTech). We changed medium every other day by carefully replacing the supernatant with fresh medium containing 20 ng/mL GM-CSF. We harvested semi-adherent BMDCs on day seven unless stated differently. If not stated differently, we refer to GM-CSF-derived BMDCs as BMDCs. M-CSF-induced BMDC were generated by culturing BMDC in six well-plates (Sarstedt) containing 20 ng/mL M-CSF (PeproTech). We added every other day, half of the starting volume containing 20 ng/mL M-CSF. We harvested adherent cells on day seven after incubating with Accutase (PAN Biotech) for 20 min at 37°C. Flt3-ligand-induced BMDC were generated by culturing BMDC in six well-plates (Sarstedt) containing 100 ng/mL Flt3L (PeproTech). We harvested semi-adherent cells on day seven.

Mixed bone marrow chimeras

We sublethally irradiated mice with one dose of 9.5 Gy (Biobeam). Twenty-four hours later, we i.v. injected mice with 2–3 × 10^6 naïve bone marrow cells from WT CD45.1 or *Arc/Arg3.1*^{eGFP} mice [53]. After one to six weeks, we collected sdLN, spleen, bone marrow, and ears, processed them as described above and analyzed them in comparison to naïve WT or *Arc/Arg3.1*^{eGFP} mice using flow cytometry.

DC precursors in vitro

We fluorescently sorted DC precursors from bone marrow of naïve CD45.2 *Arc/Arg3.1*^{eGFP} mice with a purity of at least 95% using FACS ARIA IIIu (BD Biosciences). We incubated 10–20 $\times$ 10^3 precursors together with 1–1.5 $\times$ 10^6 CD45.1 WT naïve bone marrow cells, under above-mentioned conditions and processed as described above. As control, only 1.5 $\times$ 10^6 bone marrow cells from naïve WT or naïve *Arc/Arg3.1*^{eGFP} mice were cultured alone. We harvested semi adherent BMDCs on day six and analyzed cells by flow cytometry.

DC transfer in vivo

We fluorescently isolated CDPs from bone marrow of naïve CD45.2 *Arc/Arg3.1*^{eGFP} mice. We anaesthetized WT CD45.1 mice and disinfected the knee with 70% ethanol. We injected approximately 3 $\times$ 10^4 CDPs via insulin syringe (BD). Four days after transfer, we analyzed sdLN by flow cytometry.

In vivo DC migration

We anaesthetized mice for 5 min and painted ears with 10 μL of 0.5% TRITC (Sigma-Aldrich) dissolved in 10% DMSO (Applichem) in a carrier solution of acetone/dibutylphthalate (1:1 Sigma-Aldrich and J.T. Barker) adapted from [1], [33]. After 48 hours or 72 hours, we collected draining cervical LN and nondraining inguinal LN, processed tissue to obtain single cell suspensions as described above, stained as described later and analyzed cells by flow cytometry. Normalized migration was calculated for migDC subsets by dividing percentage of TRITC$^+$ cells among Arc/Arg3.1$^+$ migDCs by percentage of TRITC$^+$ cells among Arc/Arg3.1$^-$ migDCs.

Staphylococcus aureus infection

We infected mice adapted from published protocols [5, 35, 36, 41]. In detail, we shaved mice on the abdomen under anesthesia. We grew *Staphylococcus aureus* SH1000 [36] overnight in 50 mL brain heart infusion broth (Sigma-Aldrich) at 37°C while shaking at 125 rpm. The next day, we diluted 2.5 mL of the culture 1:100 and cultured it at 37°C until mid-log phase was reached. We centrifuged bacteria for 10 min at 400 rpm, washed them twice with PBS, adjusted to 1–2 $\times$ 10^9 CFU, verified by plating on LB agar (Invitrogen) and froze them until usage at –80°C. We injected 2 $\times$ 10^6 CFU in 20 μL PBS or PBS alone intradermally using insulin syringe (BD Biosciences). Every day, we photographed (Nikon Coolpix) mice and calculated lesion size using imageJ. After 4 days, we took inguinal sdLN and incubated single cell suspensions with 100 ng/mL phorbol-12-myristate-13-acetate (PMA; Sigma-Aldrich) and 1 μg/mL ionomycin (Sigma-Aldrich) in mouse complete medium for five hours. After two hours of restimulation, we added 1:500 brefeldin A (Biolegend) for the remaining time. Stimulated cells were washed, stained, and analyzed by flow cytometry.

Listeria monocytogenes infection

We adapted the protocol from [54]. Briefly, we infected mice i.v. with 1 $\times$ 10^4 bacteria of an ovalbumin recombinant *Listeria monocytogenes* strain, as described before [55]. Eight days postinfection, we stimulated spleen cells ex vivo for 4 hours with 10^{-5} M of the listeriolysin O peptide $LLO_{189–201}$ and 10^{-6} M of the ovalbumin peptide $OVA_{257–264}$, or we incubated without stimulation [56]. After 30 min, we added 10 μg/mL brefeldin A. Subsequently, we stained cells for surface markers and intracellular cytokines and analyzed by flow cytometry.

OT-I and OT-II assay

We cocultured 2 $\times$ 10^5 MACS purified OT-ll CD4$^+$ T cells (>95% purity; negatively enriched; Miltenyi Biotec) after staining them with proliferation dye eFluor647 (eBioscience) with 10^3 FACS sorted living MHCll^{high}CD11c$^+$CD11b^{int}Arc/Arg3.1-eGFP-pos. or neg. BMDCs from *Arc/Arg3.1*^{eGFP} mice (>96% purity) in the presence of 10 μg $Ova_{323-339}$ peptide (Preprotech), 10 μg Ova protein or 20 μg Ova protein (Sigma-Aldrich) in 200 μL RPMI complete. We purified and stained OT-l CD8$^+$ T cells as described above and co-cultured 2 $\times$ 10^5 CD8$^+$ T cells with 1 $\times$ 10^3 peptide pulsed eGFP$^+$ and eGFP$^-$ sorted BMDCs (10, 1, or 0.1 ng $Ova_{257–264}$ peptide (Preprotech) at 37°C for 30 min) in 200 μL RPMI complete. For controls, we cultured unpulsed sorted BMDCs in the presence of 150 or 50 μg Ova protein. For further controls for both assays, we cultured T cells without BMDCs or with anti-CD3 and anti-CD28. Cell count, surface expression, and cell proliferation were analyzed by flow cytometry after 96 hours.

Quantitative real-time PCR (qRT-PCR) for measuring mRNA expression

We purified RNA with RNeasy Mini or Micro Kit (Qiagen) and synthesized cDNA with RevertAid H Minus First Strand cDNA Synthesis Kit (Fermentas) and diluted cDNA 1:5 in H_2O for analysis. For quantitative real-time PCR, we used TaqMan Gene Expression Assays (LifeTechnologies) and performed all analyses in triplicates: Mm01204954_g1 (mouse *Arc*, sample) Mm00801709_m1 and TATA-binding protein as endogenous control Mm00446971_m1 (mouse *tbp*, reference). In some qRT-PCR we used Universal ProbeLibrary from Roche with Arc/Arg3.1 (fw: GGT GAG CTG AAG CCA CCA AT, rw: TTC ACT GGT ATG AAT CAC TGC TG; Biomers) and normalized to *b-actin* (05046190001). We analyzed all samples with a 7900HT Fast Real-Time PCR System (Applied Biosystems) and used SDS v2.4 and RQ Manager software for analysis. Gene expression of

genes of interest was calculated as $2^{-\Delta CT}$ relative to *Tbp*, *b-actin* or calculated as $2^{-\Delta\Delta CT}$ relative to mean *Arc/Arg3.1* expression of GM-CSF generated BMDC sample.

Flow cytometry

We excluded dead cells by staining with LIVE/DEAD Fixable Aqua or Near-IR Dead Cell Stain Kit (Life Technologies) following manufacturer's protocols. Afterwards, we incubated cells with antibody for 30 min at 4°C: CD3 (17A2; BioLegend), CD3 (145-2C11; eBioscience), CD4 (RM4-5; BioLegend), CD8a (53-6.7; BioLegend), CD11b (M1/70; BioLegend), CD11c (N418; BioLegend), CD19 (6D5; BioLegend), CD16/32 (93; eBioscience), CD24 (M1/69; BioLegend), CD40 (3/23; BioLegend), CD40L (MR1; eBiosciences), CD44 (30F11; BioLegend), CD45 (30F11; BioLegend), CD45R (RA3-6B2; eBioscience), CD45.1 (A20; BioLegend), CD45.2 (104; BioLegend), CD103 (2E7; BioLegend), CD115 (AFS98; eBioscience), CD115 (AFS98; BioLegend), CD117 (2B8; BioLegend), CD135 (A2F10; BioLegend), Ly-6C (HK1.4; BioLegend), MHCII (M5/114.15.2; BioLegend), NK1.1 (PK136; BioLegend), Ter119 (TER-119; BioLegend). For gating on Arc/Arg3.1-eGFP$^+$ cells, we always used a respective WT control. For intracellular stainings, after LIVE/DEAD and surface staining, we washed cells and performed fixation and permeabilization with IC fixation and permeabilization buffer (eBioscience). We stained intracellular cytokines with anti-IL17A (eBio17B7; eBioscience), IFN-γ (XMG1.2; eBioscience or BD Biosciences) and TNF-α (MP6-XT22; BioLegend) for 20 min at RT. We washed stained cells with permeabilization buffer (1500 rpm, 5 min, RT) and resuspended in 300 μL FACS buffer. A mouse Anti-Arc/Arg3.1 antibody (generous gift from Paul Worley, Baltimore) was labeled directly with DyLight 650, after surface staining, intracellular staining (for 45 min) with the FoxP3 staining buffer set (eBioscience). For gating on Arc/Arg3.1$^+$ cells, we always used a respective *Arc/Arg3.1*$^{-/-}$ control. We quantified cells using TrueCOUNT beads (BD Biosciences). We used a BD LSR II flow cytometer (BD Biosciences) and analyzed data with FlowJo (Tree Star). When possible, the rater was blinded for genotype and/or condition. Cell sorting was performed on BD FACS ARIA IIIu (BD Biosciences).

GM-CSF injection

WT mice were subcutaneously injected into the flank with 5 μg GM-CSF (Peprotech) in 100 μL PBS or PBS only for five consecutive days according to [57]. At day 6 inguinal LN were analyzed by flow cytometry.

Immune cell identification strategies

For flow cytometry analysis and fluorescent cell sorting, we identified immune cell subsets in sdLN and skin (unless depicted differently) from LiveCD45$^+$Singlets: B cells (CD19$^+$CD3$^-$); T cells (CD3$^+$CD19$^-$); DCs (CD11c$^+$CD19$^-$CD3$^-$); migratoryDCs: complete (SSC^{high}FSC^{high}MHCII^{high}CD11c^{inter}), CD11b$^+$ migratoryDCs (CD11b$^+$CD24$^-$), dnDCs (CD11b$^-$CD24$^-$), CD103$^+$DCs (CD11b$^{-/int}$CD24$^+$CD103$^+$), CD103$^-$DCs + LC (CD11b$^{-/int}$CD24$^+$CD103$^-$); classical DCs (SSC^{high}FSC^{high}CD11c^{high}MHCII^{inter}); plasmacytoid DCs (CD11c^{inter}PDCA1$^+$); lymphocytes (FSC^{low}SSC^{low} autoflourescence$^-$CD45$^+$CD11c$^-$); CDPs (Lin$^-$(NK1.1, TER119, CD3, CD19)MHCII$^-$CD11c$^-$CD11b$^-$CD115$^+$CD117$^-$CD135$^+$); MDPs (Lin$^-$(NK1.1, TER119, CD3, CD19)MHCII$^-$CD11c$^-$CD11b$^-$CD115$^+$CD117$^+$CD135$^+$); cMOPs (Lin$^-$(NK1.1, TER119, CD3, CD19)MHCII$^-$CD11c$^-$CD11b$^-$CD115$^+$CD117$^+$CD135$^-$Ly6c$^+$), and naïve Arc/Arg3.1-eGFP$^+$ (SSC^{int}FSC^{int}Arc/Arg3.1-eGFP$^+$ Amcyan$^-$).

Statistical analysis

We performed all statistical tests using GraphPad Prism. Values are expressed as means ± SEM unless stated differently. Where indicated, we analyzed for significance by using ANOVA with appropriate posthoc analysis for multiple groups, by two-sided Student´s *t*-test or one-sample *t*-test. We considered $p < 0.05$ (*) as significant, $p < 0.01$ (**) and $p < 0.001$ (***) as highly significant.

Acknowledgments: We thank Paul Worley, Baltimore, USA, for providing anti-Arc/Arg3.1 antibody; Dietmar Kuhl, Hamburg, Germany for providing *Arc/Arg3.1*$^{-/-}$ mice, Kai Hildner, Erlangen, Germany for providing *Batf3*$^{-/-}$ mice, Panagiotis Tsapogas, Basel, Switzerland for providing *Flt3l*$^{-/-}$ mice and Eva Medina, Braunschweig, Germany for sharing *S. aureus* SH1000 with us. We are grateful to the animal facility from Universitätsklinikum Hamburg-Eppendorf for taking good care of our mice. This work was supported by the Boehringer Ingelheim Stiftung (Exploration Grant).

Author contributions: J.T. and F.U. organized, designed and performed most of the experimental work, data analysis, and wrote the manuscript. H.W. performed some BMDC experiments. J.B.E. helped with statistics and writing of the manuscript. K.L. and H.W.M. carried out experiments with *Listeria monocytogenes*. M.A.F. oversaw the experiments, provided funding for the research, and wrote the manuscript.

Conflict of interest: The authors declare no commercial or financial conflict of interest.

References

1 **Tamoutounour, S., Guilliams, M., MontananaSanchis, F., Liu, H., Terhorst, D., Malosse, C., Pollet, E. et al.**, Origins and functional

specialization of macrophages and of conventional and monocyte-derived dendritic cells in mouse skin. *Immunity* 2013. **39**: 925–938.

2 **Mildner, A. and Jung, S.**, Development and function of dendritic cell subsets. *Immunity* 2014. **40**: 642–656.

3 **Malissen, B., Tamoutounour, S. and Henri, S.**, The origins and functions of dendritic cells and macrophages in the skin. *Nat. Rev. Immunol.* 2014. **14**: 417–428.

4 **Pulendran, B.**, The varieties of immunological experience: of pathogens, stress, and dendritic cells. *Annu. Rev. Immunol.* 2015. **33**: 563–606.

5 **Naik, S., Bouladoux, N., Linehan, J. L., Han, S.-J., Harrison, O. J., Wilhelm, C., Conlan, S. et al.**, Commensal–dendritic-cell interaction specifies a unique protective skin immune signature. *Nature* 2015. **520**: 104–108.

6 **Igyártó, B. Z., Haley, K., Ortner, D., Bobr, A., Gerami-Nejad, M., Edelson, B. T., Zurawski, S. M. et al.**, Skin-resident murine dendritic cell subsets promote distinct and opposing antigen-specific T helper cell responses. *Immunity* 2011. **35**: 260–272.

7 **Clausen, B. E. and Stoitzner, P.**, Functional specialization of skin dendritic cell subsets in regulating T cell responses. *Front. Immunol.* 2015. **6**: 1–19.

8 **Ginhoux, F., Liu, K., Helft, J., Bogunovic, M., Greter, M., Hashimoto, D., Price, J. et al.**, The origin and development of nonlymphoid tissue CD103 $^{+}$ DCs. *J. Exp. Med.* 2009. **206**: 3115–3130.

9 **Liu, K., Victora, G. D., Schwickert, T. A., Guermonprez, P., Meredith, M. M., Yao, K., Chu, F.-F. et al.**, In vivo analysis of dendritic cell development and homeostasis. *Science* 2009. **392**: 392–397.

10 **Naik, S. H., Sathe, P., Park, H.-Y., Metcalf, D., Proietto, A. I., Dakic, A., Carotta, S. et al.**, Development of plasmacytoid and conventional dendritic cell subtypes from single precursor cells derived in vitro and in vivo. *Nat. Immunol.* 2007. **8**: 1217–1226.

11 **Kingston, D., Schmid, M. A., Onai, N., Obata-onai, A., Baumjohann, D. and Manz, M. G.**, The concerted action of GM-CSF and Flt3-ligand on in vivo dendritic cell homeostasis. *Blood* 2009. **114**: 1–3.

12 **Onai, N., Obata-Onai, A., Tussiwand, R., Lanzavecchia, A. and Manz, M. G.**, Activation of the Flt3 signal transduction cascade rescues and enhances type I interferon–producing and dendritic cell development. *J. Exp. Med.* 2006. **203**: 227–238.

13 **Tussiwand, R., Onai, N., Mazzucchelli, L. and Manz, M. G.**, Inhibition of natural type I IFN-producing and dendritic cell development by a small molecule receptor tyrosine kinase inhibitor with Flt3 affinity. *J. Immunol.* 2005. **175**: 3674–3680.

14 **Gomez Perdiguero, E., Klapproth, K., Schulz, C., Busch, K., Azzoni, E., Crozet, L., Garner, H. et al.**, Tissue-resident macrophages originate from yolk-sac-derived erythro-myeloid progenitors. *Nature* 2014. **518**: 547–551.

15 **Merad, M., Manz, M. G., Karsunky, H., Wagers, A., Peters, W., Charo, I., Weissman, I. L. et al.**, Langerhans cells renew in the skin throughout life under steady-state conditions. *Nat. Immunol.* 2002. **3**: 1135–1141.

16 **Inaba, K., Inaba, M., Romani, N., Aya, H., Deguchi, M., Ikehara, S., Muramatsu, S. et al.**, Generation of large numbers of dendritic cells from mouse bone marrow cultures supplemented with granulocyte/macrophage colony-stimulating factor. *J. Exp. Med.* 1992. **176**: 1693–1702.

17 **Sallusto, B. F. and Lanzavecchia, A.**, Efficient presentation of soluble antigen by cultured human dendritic cells is maintained by granulocyte/macrophage colony-stimulating factor plus interleukin 4 and down-regulated by tumor necrosis factor alpha. *J. Exp. Med.* 1994. **179**: 1109–1118.

18 **Lacey, D. C., Achuthan, A., Fleetwood, A. J., Dinh, H., Roiniotis, J., Scholz, G. M., Chang, M. W. et al.**, Defining GM-CSF- and macrophage-CSF-dependent macrophage responses by in vitro models. *J. Immunol.* 2012. **188**: 5752–5765.

19 **Helft, J., Böttcher, J., Chakravarty, P., Zelenay, S., Huotari, J., Schraml, B. U., Goubau, D. et al.**, GM-CSF mouse bone marrow cultures comprise a heterogeneous population of CD11c+MHCII+ macrophages and dendritic cells. *Immunity* 2015. **42**: 1197–1211.

20 **Hettinger, J., Richards, D. M., Hansson, J., Barra, M. M., Joschko, A.-C., Krijgsveld, J. and Feuerer, M.**, Origin of monocytes and macrophages in a committed progenitor. *Nat. Immunol.* 2013. **14**: 821–830.

21 **Sathe, P., Metcalf, D., Vremec, D., Naik, S. H., Langdon, W. Y., Huntington, N. D., Wu, L. et al.**, Lymphoid tissue and plasmacytoid dendritic cells and macrophages do not share a common macrophage-dendritic cell-restricted progenitor. *Immunity* 2014. **41**: 104–115.

22 **Paul, F., Arkin, Y., Giladi, A., Jaitin, D. A., Kenigsberg, E., Keren-Shaul, H., Winter, D. et al.**, Transcriptional heterogeneity and lineage commitment in myeloid progenitors. *Cell* 2015. **163**: 1663–1677.

23 **Hildner, K., Edelson, B. T., Purtha, W. E., Diamond, M., Matsushita, H., Kohyama, M., Calderon, B. et al.**, Batf3 deficiency reveals a critical role for CD8 + dendritic cells in cytotoxic T cell immunity. *Science* 2008. **322**: 1097–1100.

24 **Bajana, S., Roach, K., Turner, S., Paul, J. and Kovats, S.**, IRF4 promotes cutaneous dendritic cell migration to lymph nodes during homeostasis and inflammation. *J. Immunol.* 2012. **189**: 3368–3377.

25 **Bajaña, S., Turner, S., Paul, J., Kovats, S., Turner, S., Paul, J., Ainsua-enrich, E. et al.**, IRF4 and IRF8 act in CD11c + cells to regulate terminal differentiation of lung tissue dendritic cells. *J. Immunol.* 2016. **196**: 1666–1677.

26 **Suzuki, S., Honma, K., Matsuyama, T., Suzuki, K., Toriyama, K., Akitoyo, I., Yamamoto, K. et al.**, Critical roles of interferon regulatory factor 4 in CD11bhighCD8alpha-dendritic cell development. *Proc. Natl. Acad. Sci. USA* 2004. **101**: 8981–8986.

27 **Guilliams, M., Ginhoux, F., Jakubzick, C., Naik, S. H., Onai, N., Schraml, B. U., Segura, E. et al.**, Dendritic cells, monocytes and macrophages: a unified nomenclature based on ontogeny. *Nat. Rev. Immunol.* 2014. **14**: 571–578.

28 **Guilliams, M. and van de Laar, L.**, A hitchhiker's guide to myeloid cell subsets: practical implementation of a novel mononuclear phagocyte classification system. *Front. Immunol.* 2015. **6**: 1–12.

29 **Ufer, F., Vargas, P., Engler, J. B., Tintelnot, J., Schattling, B., Winkler, H., Bauer, S. et al.**, Arc/Arg3.1 governs inflammatory dendritic cell migration from the skin and thereby controls T cell activation. *Sci. Immunol.* 2016. **1**: eaaf8665–eaaf8665.

30 **Merad, M., Sathe, P., Helft, J., Miller, J. and Mortha, A.**, The dendritic cell lineage: ontogeny and function of dendritic cells and their subsets in the steady state and the inflamed setting. *Annu. Rev. Immunol.* 2013. **31**: 563–604.

31 **Gong, S., Zheng, C., Doughty, M. L., Losos, K., Didkovsky, N., Schambra, U. B., Nowak, N. J. et al.**, A gene expression atlas of the central nervous system based on bacterial artificial chromosomes. *Nature* 2003. **425**: 917–925.

32 **King, I. L., Kroenke, M. A. and Segal, B. M.**, GM-CSF–dependent, CD103 $^{+}$ dermal dendritic cells play a critical role in Th effector cell differentiation after subcutaneous immunization. *J. Exp. Med.* 2010. **207**: 953–961.

33 **Gomez de Agüero, M., Vocanson, M., Hacini-Rachinel, F., Taillardet, M., Sparwasser, T., Kissenpfennig, A., Malissen, B. et al.**, Langerhans cells protect from allergic contact dermatitis in mice by tolerizing CD8 (+) T cells and activating Foxp3 (+) regulatory T cells. *J. Clin. Invest.* 2012. **122**: 1700–1711.

34 **Tamura, T., Tailor, P., Yamaoka, K., Kong, H. J., Tsujimura, H., O'Shea, J. J., Singh, H. et al.**, IFN regulatory factor-4 and -8 govern dendritic cell subset development and their functional diversity. *J. Immunol.* 2005. **174**: 2573–2581.

35 **Cho, J. S., Zussman, J., Donegan, N. P., Ramos, R. I., Garcia, N. C., Uslan, D. Z., Iwakura, Y. et al.**, Noninvasive in vivo imaging to evaluate immune responses and antimicrobial therapy against *Staphylococcus aureus* and USA300 MRSA skin infections. *J. Invest. Dermatol.* 2011. **131**: 907–915.

36 **Tebartz, C., Horst, S. A., Sparwasser, T., Huehn, J., Beineke, A., Peters, G. and Medina, E.**, A major role for myeloid-derived suppressor cells and a minor role for regulatory T cells in immunosuppression during *Staphylococcus aureus* infection. *J. Immunol.* 2015. **194**: 1100–1111.

37 **Kaplan, D. H.**, Ontogeny and function of murine epidermal Langerhans cells. *Nat. Immunol.* 2017. **18**: 1068–1075.

38 **Guilliams, M. and Scott, C. L.**, Does niche competition determine the origin of tissue-resident macrophages? *Nat. Rev. Immunol.* 2017. **17**: 451–460.

39 **Worbs, T., Hammerschmidt, S. I. and Förster, R.**, Dendritic cell migration in health and disease. *Nat. Rev. Immunol.* 2017. **17**: 30–48.

40 **Belkaid, Y. and Hand, T. W.**, Role of the microbiota in immunity and inflammation. *Cell* 2014. **157**: 121–141.

41 **Miller, L. S., O'Connell, R. M., Gutierrez, M. A., Pietras, E. M., Shahangian, A., Gross, C. E., Thirumala, A. et al.**, MyD88 mediates neutrophil recruitment initiated by IL-1R but not TLR2 activation in immunity against *Staphylococcus aureus*. *Immunity* 2006. **24**: 79–91.

42 **Bröker, B., Mrochen, D. and Péton, V.**, The T cell response to *Staphylococcus aureus*. *Pathogens* 2016. **5**: 31.

43 **Campisi, L., Soudja, S. M. H., Cazareth, J., Bassand, D., Lazzari, A., Brau, F., Narni-Mancinelli, E. et al.**, Splenic CD8a+ dendritic cells undergo rapid programming by cytosolic bacteria and inflammation to induce protective CD8+ T-cell memory. *Eur. J. Immunol.* 2011. **41**: 1594–1605.

44 **Cohn, L., Chatterjee, B., Esselborn, F., Smed-Sörensen, A., Nakamura, N., Chalouni, C., Lee, B.-C. et al.**, Antigen delivery to early endosomes eliminates the superiority of human blood BDCA3$^+$ dendritic cells at cross presentation. *J. Exp. Med.* 2013. **210**: 1049–1063.

45 **Plath, N., Ohana, O., Dammermann, B., Errington, M. L., Schmitz, D., Gross, C., Mao, X. et al.**, Arc/Arg3.1 is essential for the consolidation of synaptic plasticity and memories. *Neuron.* 2006. **52**: 437–444.

46 **Mittrucker, H.-W.**, Requirement for the transcription factor LSIRF/IRF4 for mature B and T lymphocyte function. *Science* 1997. **275**: 540–543.

47 **Huang, R. and Kumagai, T.**, Stability and instability of Gaussian heat kernel estimates for random walks among time-dependent conductances. *Electron. Commun. Probab.* 2016. **21**: 3489–3497.

48 **Hogquist, K. A., Jameson, S. C., Heath, W. R., Howard, J. L., Bevan, M. J. and Carbone, F. R.**, T cell receptor antagonist peptides induce positive selection. *Cell* 1994. **76**: 17–27.

49 **Barnden, M. J., Allison, J., Heath, W. R. and Carbone, F. R.**, Defective TCR expression in transgenic mice constructed using cDNA- based α- and β-chain genes under the control of heterologous regulatory elements. *Immunol. Cell Biol.* 1998. **76**: 34–40.

50 **Siegert, S., Cabuy, E., Scherf, B. G., Kohler, H., Panda, S., Le, Y.-Z., Fehling, H. J. et al.**, Transcriptional code and disease map for adult retinal cell types. *Nat. Neurosci.* 2012. **15**: 487–495.

51 **Steinbach, K., Piedavent, M., Bauer, S., Neumann, J. T. and Friese, M. A.**, Neutrophils amplify autoimmune central nervous system infiltrates by maturing local APCs. *J. Immunol.* 2013. **191**: 4531–4539.

52 **Henri, S., Poulin, L. F., Tamoutounour, S., Ardouin, L., Guilliams, M., de Bovis, B., Devilard, E. et al.**, CD207$^+$ CD103$^+$ dermal dendritic cells cross-present keratinocyte-derived antigens irrespective of the presence of Langerhans cells. *J. Exp. Med.* 2010. **207**: 189–206.

53 **Schraml, B. U., Van Blijswijk, J., Zelenay, S., Whitney, P. G., Filby, A., Acton, S. E., Rogers, N. C. et al.**, Genetic tracing via DNGR-1 expression history defines dendritic cells as a hematopoietic lineage. *Cell* 2013. **154**: 843–858.

54 **Foulds, K. E., Zenewicz, L. A., Shedlock, D. J., Jiang, J., Troy, A. E. and Shen, H.**, Cutting edge: CD4 and CD8 T cells are intrinsically different in their proliferative responses. *J. Immunol.* 2002. **168**: 1528–1532.

55 **Raczkowski, F., Ritter, J., Heesch, K., Schumacher, V., Guralnik, A., Hocker, L., Raifer, H. et al.**, The transcription factor interferon regulatory factor 4 is required for the generation of protective effector CD8+ T cells. *Proc. Natl. Acad. Sci.* 2013. **110**: 15019–15024.

56 **Mahnke, J., Schumacher, V., Ahrens, S., Käding, N., Feldhoff, L. M., Huber, M., Rupp, J. et al.**, Interferon regulatory factor 4 controls TH1 cell effector function and metabolism. *Sci. Rep.* 2016. **6**: 35521.

57 **Pulendran, B., Smith, J. L., Caspary, G., Brasel, K., Pettit, D., Maraskovsky, E. and Maliszewski, C. R.**, Distinct dendritic cell subsets differentially regulate the class of immune response in vivo. *Proc. Natl. Acad. Sci. USA* 1999. **96**: 1036–1041.

Abbreviations: **cMOP**: common monocyte precursors · **dLN**: draining lymph nodes · **LC**: Langerhans cells · **MDP**: monocyte-DC precursor · **TRITC**: tetramethyl rhodamine isothiocyanate

Full correspondence: Prof. Manuel A. Friese, Institut für Neuroimmunologie und Multiple Sklerose, Zentrum für Molekulare Neurobiologie Hamburg, Universitätsklinikum Hamburg Eppendorf, Falkenried 94, 20251 Hamburg, Germany
e-mail: manuel.friese@zmnh.uni-hamburg.de

The peer review history for this article is available at https://publons.com/publon/10.1002/eji.201847797

Received: 6/7/2018
Revised: 14/12/2018
Accepted: 18/2/2019
Accepted article online: 20/2/2019

